Electrohydrodynamics of Dye Molecules in an Isotropic Liquid Crystal Studied by the Transient Grating Method

Daeseong Jin and Hackjin Kim*

Department of Chemistry, Chungnam National University, Taejon, 305-764, Korea

Sun Hee Kim and Seong Kyu Kim

Department of Chemistry, Sung Kyun Kwan University, Suwon, 440-746, Korea

Received: October 7, 1996; In Final Form: September 8, 1997[⊗]

The transient grating method using a nanosecond laser pulse as the pump and a CW laser beam as the probe is applied to a dye (methyl red)-doped isotropic liquid crystal (MBBA) under a dc electric field. The diffracted signal decays biexponentially due to the faster (in the μs time scale) heat diffusion and the slower (in the ms time scale) mass diffusion of the dye molecule at zero electric field. No significant changes of the heat diffusion by the electric field are observed. The decay by the mass diffusion is greatly affected by the electric field, but the electrohydrodynamic convective flow is not observed. The complementary grating effect is observed in the mass diffusion under the weak electric field, which is explained well with the hydrodynamic model. The viscosity of the medium and the solute−solvent interactions are affected by the electric field. The activation energy of diffusion, which corresponds to the activation energy of viscosity in the hydrodynamic model, decreases with the electric field. The intermolecular association of methyl red and MBBA increases under the electric field so that the diffusional friction grows. The viscosity decrease by the electric field gives greater effect on the diffusion than the diffusional friction due to intermolecular association. Therefore, the diffusion becomes faster under the electric field.

Introduction

The transient grating (TG) method is one of the sensitive spectroscopic techniques for studying various molecular motions and transport processes.[1] Molecular reorientation in solution[2] and relaxation of local structures in liquids[3] have been studied by the TG method using picosecond or shorter laser pulses. Examples of transport processes investigated by the TG method are electron transfer,[4] excited electronic-state transport,[5] propagation of acoustic waves,[6] and diffusion of atoms in flames.[7] A great advantage of the TG method for the studies of transport processes is the reduction of the diffusion length to a few micrometers so that the diffusion time decreases considerably. The TG method with nanosecond-pulsed lasers or chopped CW lasers has been used to investigate transport processes in the microsecond or longer time scales. These include thermal diffusion in condensed phases,[8] diffusion of dye molecules in polymeric solutions[9−11] and liquid crystals,[12−15] and diffusion of radical intermediates produced from photochemical reactions.[16] The TG signals usually show the exponential decay, and the decay time constant τ is related to the involved diffusion constant D and the fringe spacing d as in the following:

$$1/\tau = 1/\tau_{rec} + 4\pi^2 D/d^2 = 1/\tau_{rec} + Dq^2 \qquad (1)$$

where τ_{rec} is the recovery time of the photoconverted form of the diffusing species and q ($=2\pi/d$) is the grating wave vector. The fringe spacing is given by the Bragg condition $d = \lambda/[2 \sin(\theta/2)]$ where λ is the excitation laser wavelength and θ is the crossing angle of two excitation laser beams. The diffusion constant can be determined accurately from the fringe spacing dependence of the dynamics.

In this work, we apply the TG method for a dye-doped isotropic liquid crystal under a dc electric field in order to study the effects of the electric field on the diffusion dynamics in the isotropic liquid crystal. Although the electric field is widely used for the liquid crystal devices,[17] the electric field effects on the dynamics of liquid crystals are not well understood. We use methyl red (MR) as the dopant dye molecule in MBBA (4-methoxybenzylidene-4-*n*-butylaniline), which is one of the most widely studied liquid crystal molecules. MR is a widely used probe molecule for the TG method in various liquids,[18,19] polymeric solutions[9−11] and matrixes,[20] and liquid crystals.[12−15,21] MR has the trans form in the dark but converts to the cis form with illumination of wavelengths shorter than 590 nm.[22] According to a model of the photoisomerization of azo dyes,[23] the isomerization through the electronically excited states and the relaxation to the ground state of each isomer take place within the time resolution of our experiment ($\sim$1 μs). As the light excitation in the TG method creates the bright and dark region, the heat generated from the intramolecular relaxation process induces the thermal grating and the population difference of the trans and the cis MR induces the population grating. The decay time constant of the thermal grating is related to the thermal diffusivity D_{th} given by $D_{th} = \kappa/(\rho C_p)$ where κ, ρ, and C_p are the thermal conductivity, the density, and the heat capacity of the solvent. Since the molecular shapes of MR and MBBA are similar, several groups have studied the diffusion dynamics of the MR-doped MBBA.[12−15] Anisotropic diffusion of MR in the nematic MBBA studied using the TG method with millisecond laser pulses has been reported. The self-diffusion constant of the nematic MBBA is about 40% greater than the diffusion constant of MR in the nematic MBBA. The smaller diffusion constant of MR in MBBA is attributed to the intermolecular association due to the dipole−dipole interaction rather than the hydrogen-bonding ability of MR.

One of the well-known electric field effects on the liquid crystals is the alignment of liquid crystal molecules along the external electric field, called Freedericksz transition.[24,25] Vari-

[⊗] Abstract published in *Advance ACS Abstracts,* November 15, 1997.

S1089-5647(96)03078-7 CCC: $14.00

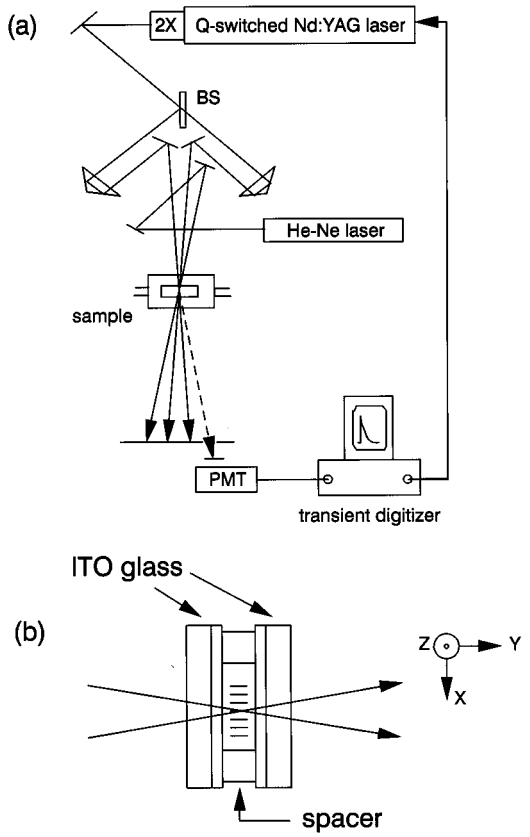

Figure 1. (a) Schematic diagram of the TG experimental setup. The second harmonic (532 nm) of a Q-switched Nd:YAG laser is split into two beams and used as the excitation pulse. The CW He−Ne laser beam is used as the probe. The diffracted probe beam is detected with a photomultiplier and a transient digitizer. (b) Sandwich type sample cell. The incident laser beams are perpendicular to the *xz* plane, and the diffusion along the *x* axis is studied.

ous electrohydrodynamic instability by the electric field are also induced in the liquid crystalline phases. The nematic liquid crystals exhibit Williams domains due to the flow driven by the electric field.[26] The electric field effects are attributed to large anisotropic properties of liquid crystalline phases. The microscopic anisotropy of the isotropic liquid crystals persists well above the nematic−isotropic transition temperature. In the isotropic phase, the alignment of the molecules along the external field and the electrohydrodynamic instabilities occur in similar manners but on different scales from the nematic phase.[25]

Experimental Section

The schematic diagram of the TG setup is shown in Figure 1a, and the details of the setup are found in ref 19. The second harmonics (532 nm, about 5 mJ/pulse) of a Q-switched Nd:YAG and a CW He−Ne laser beam (5 mW) are used as the excitation and the probe beam, respectively. The TG diffraction signal is detected with a photomultiplier tube (Hamamatsu, R928) and recorded by a transient digitizer (Gagescope, CS250). The investigated fringe spacing is in the range 2−10 μm, and typically 100 signals are averaged at a rate of 1 Hz. The sample is sandwiched between two ITO glasses with a 200 μm thick Teflon spacer as shown in Figure 1b. Since the grating wave vector is along the *x* axis and the external electric field is applied along the *y* axis, the diffusion perpendicular to the electric field direction is studied in the experiment. The sample cell is held inside a brass block whose temperature is controlled with a circulating water bath. The sample temperature is kept constant within ±0.5 °C in the range 40−85 °C.

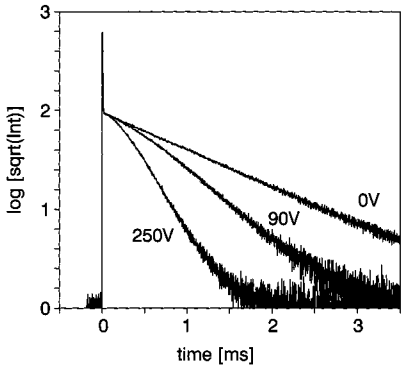

Figure 2. Decay profiles of the TG signals at 0, 90, and 250 V. The fringe spacing is 2.3 μm and temperature is 47 °C. The faster component, unaffected by the electric field, appears as a spike. The slower component relaxes more quickly under the electric field.

MBBA (Tokyo Kassei) and MR (Aldrich) are used as received. Nematic−isotropic temperature of MBBA is around 46 °C. The absorbance of the MR-doped MBBA sample is around 3 at 532 nm when the concentration of MR is about 1 $\times 10^{-3}$ M. The absorbance of the sample at 532 nm is reduced by about 10% when the sample is heated from 45 to 85 °C. Application of the dc electric field does not affect the absorption spectra of the MR-doped MBBA. The electric field effect on the decay pattern of the TG signal is reversible in the range of the applied voltage of 0−350 V.

Results and Discussion

Typical decay profiles of the TG signals at the external voltages of 0, 90, and 250 V are shown in Figure 2. At zero electric field, the signal decay is well fitted by a biexponential function with the well-separated time constants in the microsecond and millisecond regimes:

$$I(t) = [A_{\text{fast}} \exp(-t/\tau_{\text{fast}}) + A_{\text{slow}} \exp(-t/\tau_{\text{slow}})]^2 + C \quad (2)$$

where C is the incoherent background scattering. The time constant of the faster decay component is 2.1 ± 0.5 μs at the fringe spacing of 2.3 μm, independent of the applied voltage and the solvent temperature. It is attributed to the thermal grating. The thermal diffusivity of the isotropic MBBA is estimated to be (6.1 ± 1.0) $\times 10^{-4}$ cm^2/s from the fringe spacing dependence in the temperature range 45−85 °C. This value is slightly smaller than the value calculated with the thermodynamic parameters of MBBA,[27,28] which is (8.3−10.5) $\times 10^{-4}$ cm^2/s in the investigated temperature range. The difference of the experimental and the calculated thermal diffusivities may arise from the doping dye molecules.

There have been a few reports about the effects of the external electric and magnetic field on the thermal properties of the liquid crystals.[29−31] The external fields can change the sign of the anisotropy as well as the magnitude of the properties of the liquid crystals. However, it is reported that the thermal conductivity of an isotropic liquid crystal is not affected by a magnetic field.[30] The electric field effect on the thermal properties of the isotropic liquid crystals may be negligible. Photoacoustic spectroscopy by which the changes of thermal properties of a sample can be detected[32] may be required in order to investigate the electric field effects on the thermal properties of the isotropic liquid crystals in detail.

The slower decay component of the TG signal is attributed to the mass diffusion of MR. Since the refractive index modulation is induced by the population difference of both the trans and the cis isomers of MR, the single-exponential decay

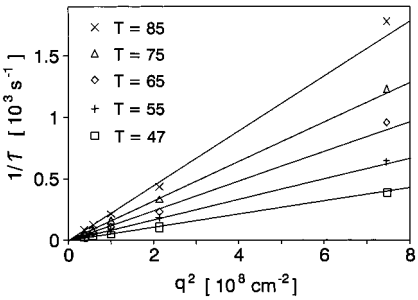

Figure 3. Fringe spacing dependence of the decay time for the mass diffusion at zero electric field in the temperature range 47−85 °C.

of the slower component at zero electric field indicates that the diffusion constants of the two isomers are identical. The deviation of the slower component from the single-exponential function under the electric field results from two out-of-phase gratings with different decay time constants. This is called a complementary grating effect,[33] which, in our case, appears as slightly different diffusion constants of the two MR isomers under the electric field. The details of the mass diffusion under the electric field including the complementary grating effect are discussed in the following section.

A. Mass Diffusion at Zero Electric Field. Figure 3 shows the fringe spacing dependence of the decay times for the mass diffusion in the temperature range 47−85 °C. The zero intercept indicates that the recovery time of the cis MR into trans MR is very long compared with the diffusion time. The recovery time of cis MR in the nematic MBBA is observed to be 64 s at 22 °C in the dark and is reduced to a few seconds under visible light.[14] The recovery time in the isotropic MBBA under the excitation laser beam is considered to be on the order of 10 s. The mass diffusion constant of MR in MBBA is determined from the slope of the plot, and it ranges from 0.3×10^{-6} to 1.3×10^{-6} cm^2/s in the investigated temperature range. These diffusion constants of MR in the isotropic MBBA agree well with the reported values, $(0.5-1.0) \times 10^{-6}$ cm^2/s [12] and $(0.5-0.8) \times 10^{-6}$ cm^2/s,[13] in the temperature range 45−60 °C. The diffusion constant of a cholesteric ester in the isotropic MBBA (0.5×10^{-6} cm^2/s)[34] is similar to the self-diffusion constants of the isotropic MBBA ($(0.6-1.0) \times 10^{-6}$ cm^2/s [12,34,35]).

According to the hydrodynamic model by Stokes and Einstein,[36] the diffusion constant D is given by

$$D = kT/(6\pi\eta R_0 f) \tag{3}$$

where k is the Boltzmann constant, T is the temperature, η is the viscosity coefficient of the solvent, R_0 is the hydrodynamic radius of the diffusing molecule, and f is the correction factor for the solute−solvent intermolecular interactions. The f value can be regarded as a friction factor in the diffusion. In the stick boundary condition, $f = 1$, and in the slip boundary condition, $f = {}^2/_3$. A spherical shape of the diffusing molecule is assumed in eq 3. The linear relation of T/η and the diffusion constant is confirmed in the diffusion of MR in the isotropic MBBA. The temperature dependence of the diffusion constant is usually expressed by the Arrhenius type equation, $D = D_0 \exp(-E_D/(RT))$, and the parameters of D_0 and E_D can be determined from the measurements of the diffusion constants in a wide temperature range. The D_0 and E_D for MR in the isotropic MBBA are 0.30 cm^2/s and 8.8 kcal/mol at zero electric field, respectively. The observed activation energy of diffusion agrees with the reported value for MR in the isotropic MBBA (10 ± 1.5 kcal/mol [10,13]). For the self-diffusion of the isotropic MBBA, the activation energy of diffusion is observed as 6.0−8.0 kcal/mol.[35,37] Discussion about the diffusion parameters under the electric field is given in the following section.

B. Mass Diffusion under the Electric Field. The orientation of the nematic liquid crystal molecules is affected by the electric field, and complex electrohydrodynamic instabilities including convection are induced by the orientation change, and various patterns of liquid crystals under the external field are produced by the instabilities.[24,25,38] Nematic liquid crystal molecules with negative dielectric anisotropy ($\epsilon_{||} < \epsilon_{\perp}$) such as MBBA align in the direction normal to the applied field direction. The alignment of MBBA molecules by the electric field makes it easy to diffuse in the plane parallel to the glass plates of Figure 1b. Therefore, the shear viscosity decreases under the electric field for the liquid crystals with the negative dielectric anisotropy. When the similar orientation change by the electric field occurs in the isotropic MBBA, the viscosity drop increases the diffusion constant as seen in eq 3.

When the convection by the electrohydrodynamic instabilities is added to the diffusion, the diffusion equation governing the TG signal is given by[39]

$$\partial N(x,t)/\partial t = D\,\partial^2 N(x,t)/\partial x^2 - v\,\partial N(x,t)/\partial x - N(x,t)/\tau_{rec} \tag{4}$$

where $N(x,t)$ is the population of the photoconverted form, D is the diffusion constant, v is the convection velocity, and τ_{rec} is the recovery time as in equation 1. Equation 1 is obtained from $v = 0$ and the initial condition $N(x,0) = (1/2)(1 + \cos qx)$.[40] Here, q is the grating wave vector as in eq 1. Since the population change along the grating wave vector affects the TG signal, one dimensional diffusion is considered above. The solution of eq 4 under the same initial condition is given by

$$N(x,t) = (1/2)\exp(-t/\tau_{rec})[1 + \exp(-q^2 Dt)\cos q(x - vt)] \tag{5}$$

and the TG signal $S(t)$ is proportional to the square of the population difference of the photoconverted form at $x = 0$ and $x = d/2$, $D(t)$.

$$\begin{aligned} S(t) \propto [D(t)]^2 &= [N(0,t) - N(d/2,t)]^2 \\ &= \exp[-2(1/\tau_{rec} + q^2 D)t]\cos^2 qvt \\ &= \exp(-2t/\tau)\cos^2 2\pi\omega t \end{aligned} \tag{6}$$

where $1/\tau = 1/\tau_{rec} + q^2 D$ and $\omega = v/d$. Equation 1 corresponds to the case $\omega = 0$ in eq 6, that is, $v = 0$ in eq 4. The decay pattern of the TG signal depends on the relative speed of the diffusion and convection along the grating wave vector. When the convection is faster than the diffusion, $2\pi\omega \gg 1/\tau$, the TG signal decays with oscillation. When the convection is slower, $2\pi\omega \ll 1/\tau$, the convection effect will not be observed in the decay of TG signal. The TG signal decays before oscillation, since $\cos^2 2\pi\omega\tau \cong 1$.

The decay patterns of Figure 2, which do not show any oscillation under the electric field, indicate that the convection in the isotropic MBBA under the electric field is very slow compared with the diffusion if it exists. The convection velocity of nematic liquid crystals under the electric field is reported to be around 10 μm/s.[41,42] When the fringe spacing is 10 μm and the signal decays to zero within 10 ms, it is not possible to observe the signal oscillation since $\cos^2[2\pi(10\ \mu\text{m/s})(10\ \text{ms})/(10\ \mu\text{m})] = 0.996$. The electrohydrodynamic convection velocity is considered to be even smaller in the isotropic liquid crystal than in the nematic liquid crystal. The anisotropic orientation of the nematic phase plays a significant role in the

generation of complex electrohydrodynamic instabilities including convection, which originate in the distortion of the director orientation under the electric field. The liquid crystals keep microscopic anisotropy well above the nematic−isotropic transition temperature. The isotropic phase of the liquid crystal consists of anisotropic droplets called pseudonematic domains, which have a correlation length shorter than 20 times of the molecular dimension.[24] Random motions of the pseudonematic domains prevent strong anisotropic interactions with the electric field. Therefore, the directional flow under the electric field such as convection, which results from the anisotropic interactions, is much slower in the isotropic phase than in the nematic phase.

The decay component due to the mass diffusion deviates from the single-exponential function under the electric field as shown in Figure 2. The observed decay pattern is attributed to the complementary grating effect from different diffusion constants of the two MR isomers as mentioned previously. The decay of the complementary grating by two out-of-phase gratings is usually described by[33]

$$I_{slow}(t) = [A_1 \exp(-t/\tau_1) - A_2 \exp(-t/\tau_2)]^2 + C \quad (7)$$

with positive A_1 and A_2. The minus sign in eq 7 implies that the two gratings are out-of-phase. Since the amplitudes and the decay time constants are related to the refractive index and the diffusion rate, the analysis of the decay pattern with eq 7 gives information about the diffusion dynamics. It is useful to recognize that the thermal grating and the population grating is in-phase. The change of the refractive index with temperature, dn/dT for the isotropic MBBA is negative[28] as for most liquid sovlents. This means that the refractive index difference due to the thermal grating Δn_{th}, defined as ($n_{bright} - n_{dark}$), is negative. Therefore, the refractive index difference due to the population grating Δn_p ($=n_{cis} - n_{trans}$) should also be negative. The refractive indexes for the MR isomers are not known. However, the refractive indexes of the isoelectronic molecules of stilbene ($n_{trans} = 1.626$ and $n_{cis} = 1.613$) and azobenzene ($n_{trans} = 1.6266$)[43] support that the refractive index change due to the isomerization of MR is negative.

The analysis of the decay pattern under the electric field gives $A_1/A_2 > 1$ and $\tau_1/\tau_2 > 1$. The ratios of A_1/A_2 and τ_1/τ_2 are 1.03 $\pm$ 0.1 as long as the applied voltage is not so high. The threshold voltage above which the ratios deviate greatly decreases at higher temperature. Deviation of the ratios is observed around 300 V at 50 °C and above 200 V at 85 °C. The transport mechanism of MR in the isotropic MBBA is considered to be the same in the electric field range where the constant ratios of A_1/A_2 and τ_1/τ_2 are observed.

The similar curvatures are reported for the diffusion of MR in polar alcohols but are absent in nonpolar solvents.[18,19] The complementary grating effect is also reported for the diffusion of MR in the polymer solvents,[9−11] but the different decay−rise−decay patterns are observed, which correspond to the case of $A_1/A_2 > 1$ and $\tau_1/\tau_2 < 1$ in eq 7. These results indicate that the trans MR isomers diffuse faster than the cis isomers in the polymer solutions, but the cis isomers diffuse faster in polar alcoholic solvents and the isotropic MBBA under the electric field. The faster diffusion of the trans isomer in the polymeric solutions is explained with the stronger intermolecular association force of the cis isomer despite the smaller size of the cis isomer. The diffusion constant of MR in polymeric solutions being much smaller than in isotropic MBBA indicates that the diffusional friction is much greater in the polymeric solutions than in pure solvents. The diffusional friction decreases in a polar medium like the dielectric friction, and the size effect of the MR isomers is observed in polar solvents. The dielectric constant of the isotropic MBBA is small (∼5),[25] but the polarity of the medium is considered to increase under the electric field.

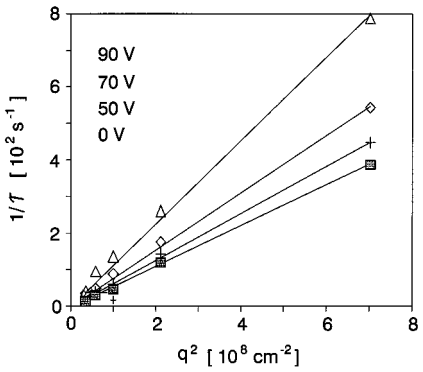

Figure 4. Decay time by the mass diffusion at 47 °C for the applied voltages lower than 100 V.

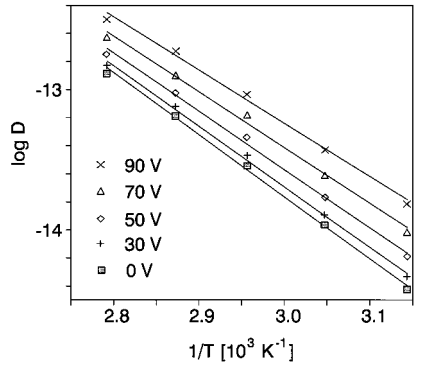

Figure 5. Temperature dependence of the mass diffusion constant at different applied voltages. The lines are the results of the least-squares fit. The Arrhenius type temperature dependence is observed, and the activation energy decreases from 8.8 to 7.5 kcal/mol when the applied voltage increases to 90 V.

The fringe spacing dependence of the mass diffusion of MR in the isotropic MBBA under the electric field is shown in Figure 4. The decay time constants are averaged values of τ_1 and τ_2 of eq 7. When the external voltage is lower than 100 V, the linear relation between $1/\tau$ and the square of the grating wave vector as given by eq 1 is observed, which indicates that the TG signal decays through diffusion. The diffusion constant, determined from the slope of the plot in Figure 4, increases with the applied field strength. Temperature dependence of the diffusion constant of MR in the isotropic MBBA under an external voltage lower than 100 V is shown in Figure 5. The activation energy of diffusion decreases with the electric field.

The effect of the electric field on the diffusion in the isotropic liquid crystal can be considered with the two parameters of eq 3: the viscosity coefficient η and the correction factor f. Modification of the local structures of the isotropic liquid crystal causes the changes of the viscosity and the solute−solvent interactions. The viscosity coefficient η depends on temperature and is frequently given by[44]

$$\eta = \eta_0 T \exp(E_\eta/(RT)) \quad (8)$$

where η_0 is a constant and E_η is the activation energy of viscosity. When the Arrhenius type temperature dependence of the diffusion constant is considered with eqs 3 and 8, we obtain $E_D = E_\eta$ and $D_0 = k(/6\pi\eta_0 R_0 f)$. The viscosity coefficient of the isotropic MBBA[45] is fit well to eq 8 with the parameters of $\eta_0 = 1.6 \times 10^{-7}$ cP/K and $E_\eta = 8.2$ kcal/mol. The activation energy of viscosity for the isotropic MBBA is close to the

TABLE 1: Diffusion Parameters and the *f* Values at Different Voltages

voltage (V)	E_D (kcal/mol)	D_0 (cm^2/s)	f_∞	f_{slope}	f_{slope}/f_∞
0	8.8 ± 0.4	0.30	0.27	0.67	2.4
30	8.6 ± 0.4	0.24	0.35	0.86	2.4
50	8.3 ± 0.4	0.17	0.50	1.23	2.5
70	7.9 ± 0.4	0.12	0.71	1.74	2.4
90	7.5 ± 0.5	0.08	1.07	2.60	2.4

activation energy for the diffusion of MR in the isotropic MBBA at zero electric field, 8.8 kcal/mol. The diffusion constants at the high-temperature limit, which correspond to the intercepts of the plots in Figure 5, decrease from 0.30 to 0.08 cm^2/s when the external voltage increases from 0 to 90 V. The parameters related with the diffusion constant are given in Table 1.

Since the activation energy of diffusion is regarded to be the same as the activation energy of viscosity, the viscosity of MBBA under the electric field can be calibrated by replacing the activation energy of viscosity with the activation energy of diffusion determined from the temperature dependence of the diffusion. As we can see below, the constant η_0 is not affected by the electric field. The activation energy of viscosity is related to the molecular interaction energy, and the constant η_0 is related to the molecular parameters,[44] which are not affected by the electric field. Figure 6 shows the plot of the inverse of the diffusion constant vs η/T where the calibrated viscosity is used. The linearity of the plot indicates that the hydrodynamic model is effective for the diffusion in the isotropic MBBA under the electric field and that the calibration of the viscosity with the activation energy of diffusion is valid.

The slope of the plot in Figure 6 corresponds to $6\pi R_0 f/k$ as seen from eq 3. In Table 1, the two *f* values estimated from the relation of $D_0 = k/(6\pi\eta_0 R_0 f)$ and the slope of the plot of Figure 6 are given as f_0 and f_{slope}, respectively. The hydrodynamic radius of 5.5 Å for MR[19] is used in the estimation of the *f* values. The f_0 value is the correction factor for the intermolecular interactions in the high-temperature limit, and the f_{slope} value represents the interaction at the experimental temperatures. Both *f* values increase with the electric field; however, the ratio of two values is invariant to the electric field. The constant ratio of f_{slope} and f_0 indicates that the constant η_0 is not affected by the electric field and that the hydrodynamic model is reasonable for the diffusion in the isotropic liquid crystal under the electric field.

When the electric field is applied through ITO glasses, MBBA molecules align in the plane parallel to the glass plates and the grating wave vector is also parallel to the glass plates. Diffusion MR molecule similar to the MBBA molecule is in the plane formed by MBBA molecules; therefore, MR molecule interacts with the host molecules more under the electric field. Greater intermolecular association of MR and MBBA molecules under the electric field leads to the increase of the diffusional friction. The change of the viscosity and the diffusional friction under the electric field give opposite effects to the mass diffusion, but the effect by the viscosity decrease is greater so that the mass diffusion accelerates under the electric field. The f_{slope} values change from 0.67 to 2.60 by a factor of 4 when the applied voltage increases to 90 V as given in Table 1. The calibrated viscosity with the activation energy of diffusion in the investigated temperature range decreases by a factor of 6 or more at 90 V.

Under the strong electric field, the ratios of A_1/A_2 and τ_1/τ_2 of eq 7 change too much to explain with the complementary grating effect and the fringe spacing dependence of the decay time constant is not fit to the one-dimensional diffusion model. However, irreversible effects such as charge injection are not observed and the decay pattern at zero electric field is reproduced whenever the electric field is removed. The dynamics under the strong electric field are responsible for complex electrohydrodynamic instabilities such as local flows, deformations, and flexoelectric effects.[24,25,38] These instabilities by the strong electric field, which require extensive theoretical and experimental studies, are too complicated to analyze from the transient grating dynamics of this work.

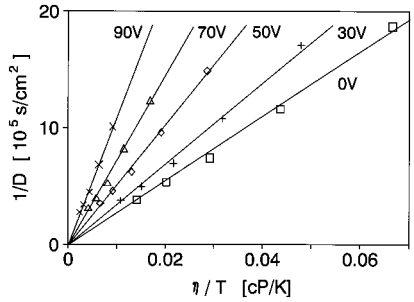

Figure 6. Inverse of the diffusion constant vs the viscosity divided by temperature at different applied voltages. The viscosity is calibrated with the activation energy of diffusion. The lines are the results of the least-squares fit. Without the calibration, the data points under the electric field shift on the line at zero electric field.

Summary

For the MR-doped isotropic MBBA, the transient grating by the nanosecond laser pulses relaxes by heat and mass diffusion. Although the heat diffusion is not affected by temperature and the electric field, the mass diffusion accelerates with temperature and the electric field. The hydrodynamic model is valid for the mass diffusion in the isotropic MBBA under the electric field. The electric field affects the viscosity of the medium and the intermolecular interactions. The activation energy of viscosity decreases under the electric field, but the diffusional friction by the intermolecular association grows with the electric field. Acceleration of the diffusion by the viscosity decrease is greater than the friction increase under the electric field so that the overall diffusion becomes faster under the electric field. The complementary grating effect by the faster diffusion of the smaller cis isomers is observed under the electric field. Electrohydrodynamic instabilities under the strong electric field produce the complex decay patterns, which cannot be analyzed with a simple one-dimensional diffusion model.

Acknowledgment. This work was supported by grants from the Basic Science Research Institute, Ministry of Education, Korea (BSRI-96-3432), the Korean Science and Engineering Foundation (94-05010-02-3), and NONDIRECT FUND of Korea Research Foundation (01 D 0587).

References and Notes

(1) Eichler, H. J.; Gunter, P.; Pohl, D. W. *Laser-Induced Dynamic Gratings*; Springer: New York, 1986.

(2) (a) Phillion, D. W.; Kuizenga, D. J.; Siegman, A. E. *Appl. Phys. Lett.* **1975**, *27*, 85. (b) Moog, R. S.; Ediger, M. D.; Boxer, S. G.; Fayer, M. D. *J. Phys. Chem.* **1982**, *86*, 4694. (c) Myers, A. B.; Hochstrasser, R. M. *IEEE J. Quantum Electron.* **1986**, *QE-22*, 1482.

(3) (a) Silence, S. M.; Duggal, A. R.; Dhar, L.; Nelson, K. A. *J. Chem. Phys.* **1992**, *96*, 5448. (b) Greenfield, S. R.; Sengupta, A.; Stankus, J. J.; Terazima, M.; Fayer, M. D. *J. Phys. Chem.* **1994**, *98*, 313. (c) Kohler, W.; Fytas, G.; Steffen, W.; Reinhardt, L. *J. Chem. Phys.* **1996**, *104*, 248.

(4) (a) Gochanour, C. R.; Andersen, H. C.; Fayer, M. D. *J. Chem. Phys.* **1979**, *69*, 4254. (b) Rose, S.; Righini, R.; Fayer, M. D. *Chem. Phys. Lett.* **1984**, *106*, 13.

(5) (a) Nelson, K. A.; Fayer, M. D. *J. Chem. Phys.* **1980**, *72*, 5202. (b) Meth, J. S.; Marshall, C. D.; Fayer, M. D. *J. Appl. Phys.* **1990**, *67*, 3362.

(6) (a) Dorfman, R. C.; Lin, Y.; Zimmt, M. B.; Baumann, J.; Domingue, R. P.; Fayer, M. D. *J. Phys. Chem.* **1988**, *92*, 4258. (b) Kasinki, J. J.; Gomez-Jahn, L. A.; Faran, K. J.; Gracewski, S. M.; Miller, R. J. D. *J. Chem. Phys.* **1989**, *90*, 1253.

(7) Fourkas, J. T.; Brewer, T. R.; Kim, H.; Fayer, M. D. *J. Chem. Phys.* **1991**, *95*, 5775.

(8) (a) Eichler, E.; Salje, G.; Stahl, H. *J. Appl. Phys.* **1973**, *44*, 5383. (b) Terazima, M. *J. Chem. Phys.* **1996**, *104*, 4988.

(9) (a) Lee, J. A.; Lodge, T. P. *J. Phys. Chem.* **1987**, *91*, 5546. (b) Lodge, T. P.; Lee, J. A.; Frick, T. S. *J. Polym. Sci.* **1990**, *B28*, 2607.

(10) (a) Xia, J. L.; Gong, S. S.; Wang, C. H. *J. Phys. Chem.* **1987**, *91*, 5805. (b) Xia, J. L.; Wang, C. H. *J. Chem. Phys.* **1988**, *88*, 5211.

(11) Lee, J.; Park, K.; Chang, T.; Jung, J. C. *Macromolecules* **1992**, *25*, 6977.

(12) Hervet, H.; Urbach, W.; Rondelez, F. *J. Chem. Phys.* **1978**, *68*, 2725.

(13) (a) Takezoe, H.; Ichikawa, S.; Fukuda, A.; Kuze, E. *Jpn. J. Appl. Phys.* **1984**, *23*, L78. (b) Hara, M.; Ichikawa, S.; Takezoe, H.; Fukuda, A. *Jpn. J. Appl. Phys.* **1984**, *23*, 1420.

(14) Urbach, W.; Hervet, H.; Rondelez, F. *J. Chem. Phys.* **1985**, *83*, 1877.

(15) Kim, S. H.; Kim, S. K.; Choi, M.; Kim, H. *Bull. Korean. Chem. Soc.* **1996**, *17*, 217.

(16) (a) Terazima, M.; Okamoto, K.; Hirota, N. *J. Phys. Chem.* **1993**, *97*, 13387. (b) Okamoto, K.; Terazima, M.; Hirota, N. *J. Chem. Phys.* **1995**, *102*, 2506. (c) Terazima, M.; Okamoto, K.; Hirota, N. *J. Chem. Phys.* **1995**, *103*, 10445.

(17) *Liquid Crystals for Advanced Technologies*; Bunning, T. J., Chen, S. H., Kajiyama, T., Koide, N., Eds.; Materials Research Society: Pittsburgh, 1996.

(18) Terazima, M.; Okamoto, K.; Hirota, N. *J. Phys. Chem.* **1993**, *97*, 5188.

(19) Kim, S. H.; Kim, S. K. *Bull. Korean. Chem. Soc.* **1996**, *17*, 365.

(20) Lee, J.; Kim, D.; Lee, M. *Appl. Opt.* **1995**, *34*, 138.

(21) (a) Eyring, G.; Fayer, M. D. *J. Chem. Phys.* **1984**, *81*, 4314. (b) Deeg, F. W.; Fayer, M. D. *J. Chem. Phys.* **1989**, *91*, 2269. (c) Deeg, F. W.; Greenfield, S. R.; Stankus, J. J.; Newell, V. J.; Fayer, M. D. *J. Chem. Phys.* **1990**, *93*, 3503. (d) Stankus, J. J.; Torre, R.; Fayer, M. D. *J. Phys. Chem.* **1993**, *97*, 9478. (e) Sengupta, A.; Fayer, M. D. *J. Chem. Phys.* **1995**, *102*, 4193. (f) Hara, M.; Takezoe, H.; Fukuda, A. *Jpn. J. Appl. Phys.* **1986**, *25*, 1756. (g) Nishikafa, T.; Minabe, J.; Takezoe, H.; Fukuda, A. *Mol. Cryst. Liq. Cryst.* **1993**, *231*, 153.

(22) (a) Ross, D. L.; Blanc, J. In *Photochromism*; Brown, G. H., Ed.; Wiley: New York, 1972; Chapter 5. (b) Griffiths, J. *J. Chem. Soc. Rev.* **1972**, *1*, 481.

(23) Zimmerman, G.; Chow, L.; Paik, U. *J. Am. Chem. Soc.* **1958**, *80*, 3528.

(24) de Gennes, P. G.; Prost, J. *The Physics of Liquid Crystals*, 2nd ed.; Clarendon: Oxford, 1993.

(25) Chandrasekhar, S. *Liquid Crystals*, 2nd ed.; Cambridge: Cambridge, U.K., 1992.

(26) (a) Williams, R. *J. Chem. Phys.* **1963**, *39*, 384. (b) Helfrich, W. *J. Chem. Phys.* **1969**, *51*, 4092.

(27) Kuss, E. *Mol. Cryst. Liq. Cryst.* **1978**, *47*, 71.

(28) Koren, G. *Phys. Rev. A* **1976**, *13*, 1177.

(29) Fisher, J.; Fredrickson, A. G. *Mol. Cryst. Liq. Cryst.* **1969**, *6*, 255.

(30) Yun, C. K.; Picot, J. J. C.; Fredrickson, A. G. *J. Appl. Phys.* **1971**, *42*, 4764.

(31) Mandelis, A.; Schoubs, E.; Paralta, S. B.; Thoen, J. *J. Appl. Phys.* **1991**, *70*, 1771.

(32) Marinelli, M.; Zammit, U.; Scudieri, F.; Martellucci, S.; Bloisi, F.; Vicari, L. *Il Nuovo Cimento* **1987**, *9D*, 855.

(33) Park, S.; Sung, J.; Kim, H.; Chang, T. *J. Phys. Chem.* **1991**, *95*, 7121.

(34) Hakemi, H.; Labes, M. M. *J. Chem. Phys.* **1974**, *61*, 4020.

(35) Ghosh, S. K.; Tettamanti, E. *Phys. Lett.* **1973**, *43A*, 361.

(36) (a) Einstein, A. *Investigations on the Theory of Brownian Motions*; Dover: New York, 1956. (b) Cussler, E. L. *Diffusion*; Cambridge: Cambridge, 1984.

(37) Ohta, K.; Terazima, M.; Hirota, N. *Bull. Chem. Soc. Jpn.* **1995**, *68*, 2809.

(38) *Pattern Formation in Liquid Crystals*; Buka, A., Kramer, L., Eds.; Springer; New York, 1996.

(39) Banks, R. B. *Growth and Diffusion Phenomena*; Springer: Berlin, 1994.

(40) Salcedo, J. R.; Siegman, A. E.; Dlott, D. D.; Fayer, M. D. *Phys. Rev. Lett.* **1978**, *41*, 131.

(41) Joets, A.; Ribotta, R. *Phys. Rev. Lett.* **1988**, *60*, 2164.

(42) Gleeson, J. T. *Nature* **1997**, *385*, 511.

(43) *CRC Handbook of Chemistry and Physics*, 75th ed.; Lide, D. R., Ed.; CRC: Boca Raton, FL, 1994.

(44) Viswanath, D. S.; Natarajan, G. *Data book on the Viscosity of Liquids*; Hemisphere: New York, 1989.

(45) Martinoty, P.; Candau, S.; Debeauvais, F. *Phys. Rev. Lett.* **1971**, *27*, 1123.